JOURNAL OF SOLID STATE CHEMISTRY 59, 272–279 (1985)

Luminescence Properties of Eu^{2+}, Sn^{2+}, and Pb^{2+} in SrB_6O_{10} and $Sr_{1-x}Mn_xB_6O_{10}$

MARKKU LESKELÄ

Department of Chemistry, University of Oulu, SF-90570 Oulu 57, Finland

TARJA KOSKENTALO

Department of Chemistry, Helsinki University of Technology, SF-02150 Espoo 15, Finland

AND GEORGE BLASSE

Physical Laboratory, State University, P.O. Box 80.000, 3508 TA Utrecht, The Netherlands

Received November 26, 1984; in revised form February 11, 1985

The luminescence properties of Eu^{2+}, Sn^{2+}, and Pb^{2+} in SrB_6O_{10} have been studied both at room-temperature and liquid-helium temperature and the decay times of Sn^{2+} and Pb^{2+} in this matrix have been measured and analyzed. According to the emission spectrum of Eu^{2+} there seems to be three different cation sites in SrB_6O_{10}. Europium, tin, and lead were also used as sensitizers for Mn^{2+} and the energy transfer processes were characterized. Eu^{2+}–Mn^{2+} energy transfer was inefficient due to the transfer within different Eu^{2+} centers. The sensitization action of Sn^{2+} and Pb^{2+} on Mn^{2+} was different because lead–lead energy transfer occurs (even at 4.2 K) but tin–tin transfer can be neglected. A fast diffusion model for the Pb^{2+} system is suggested. © 1985 Academic Press, Inc.

Introduction

Recently, the luminescence properties of Mn^{2+}-activated SrB_6O_{10} have been reported (*1*). The Sn^{2+} and Pb^{2+} ions could be used as sensitizers for Mn^{2+} and efficient phosphors were obtained in this way. Here we report the low-temperature measurements on these and the Eu^{2+}-sensitized materials. The energy transfer characteristics could be evaluated and the decay times of the sensitizers were analyzed.

Experimental

In the preparation of the samples two methods were employed from which the first has been described earlier (*1*). In the other method the starting materials were dissolved in concentrated HCl and the solution was evaporated to dryness. The precipitation was fired twice at 800°C. The firing atmosphere was air with Pb^{2+}-containing samples, nitrogen with Sn^{2+}- and hydrogen–argon mixture with Eu^{2+}-containing samples.

0022-4596/85 $3.00

Copyright © 1985 by Academic Press, Inc.
All rights of reproduction in any form reserved.

The optical measurements were carried out with a Perkin–Elmer MPF-3 fluorescence spectrometer equipped with an Oxford CF 1000 helium flow cryostat. A detailed description of the instrumentation has been presented earlier (*2*).

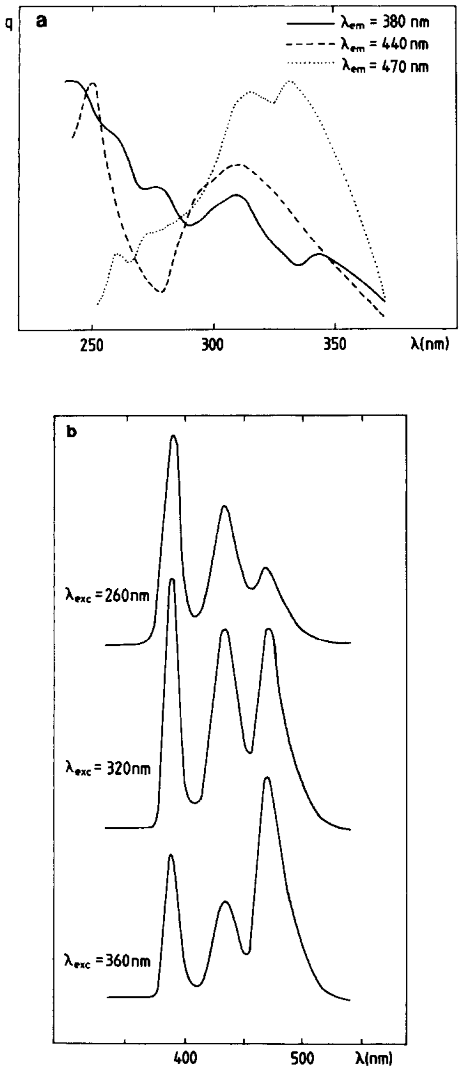

FIG. 1. The excitation (a) and emission (b) spectra of $Sr_{0.997}Eu_{0.003}B_6O_{10}$ recorded at LHeT with different wavelength combinations. In this figure as well as in all figures the excitation spectra have been corrected according to the wavelength dependence of the intensity of a Xe lamp.

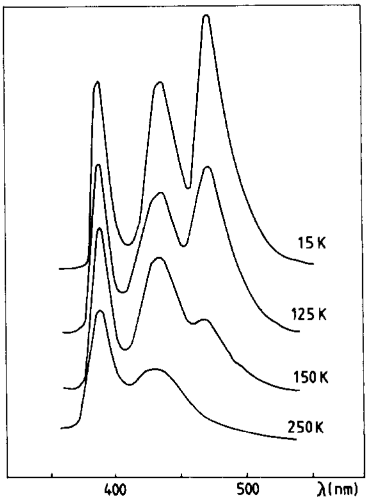

FIG. 2. The temperature dependence of the emission of different centers in $Sr_{0.997}Eu_{0.003}B_6O_{10}$. Excitation wavelength 320 nm.

Results and Discussion

1. SrB_6O_{10}:Eu^{2+}

The emission and excitation spectra of Eu^{2+}-activated SrB_6O_{10} are complicated. First we consider results of LHeT (liquid-helium temperature) (Figs. 1, 2). There are obviously three Eu^{2+} centers each with its own emission and excitation spectrum. This is summarized in Table I. At LHeT the luminescence efficiency is high. No concentration quenching was observed if samples with 0.3 and 3% of Eu^{2+} are compared. However, the emission spectra depend

TABLE I

THE POSITIONS OF THE EMISSION BANDS AND THEIR QUENCHING TEMPERATURES IN $Sr_{0.997}Eu_{0.003}B_6O_{10}$

Center	Emission wavelength (nm)	Start of excitation spectrum (nm)	T_{quench} (K)
I	~390	~375	>300
II	~435	~390	~275
III	~470	~430	~150

strongly on concentration. In the 3% Eu^{2+} sample the emission of center III is dominating. The spectral data suggest the possibility of efficient energy transfer among the different Eu^{2+} centers. Center I emits in the region where center III has an excitation band. Since we are dealing with allowed ($4f$–$5d$) transitions, transfer may occur over long distances (*3*). With a formula for the critical distance for transfer (*4*) based on Dexter's work, a value of 30 Å is estimated for R_c. Also transfer from center II to III is possible at LHeT. This suggests strongly that the increase of III emission with increasing concentration is due to transfer from the other centers to center III.

We have to conclude that the SrB_6O_{10} matrix offers three possible sites for Eu^{2+}, i.e., there are at least three cystallographic sites for Sr.

Upon increasing the temperature, the emissions are quenched in the sequence III, II, I (Fig. 2, Table I). The Stokes shift decreases in this sequence and the spectral position of the excitation spectrum will result in an increase of the thermal quenching temperature of the emission of the Eu^{2+} centers as expected from calculations by Bleijenberg and Blasse (*5*), in agreement with the experimental results.

This temperature dependence is fatal, however, for the room-temperature efficiency, especially for higher Eu^{2+} concentrations. The 3% sample, for example, shows at LHeT mainly III emission which is completely quenched at RT (room temperature). Also the emission of center II is the quenching range at RT. Consequently, concentration quenching occurs at lower concentrations at RT than at LHeT. The center III acts as a killer center at RT.

The luminescence properties of Eu^{2+}-activated SrB_6O_{10} at RT have been reported by Machida *et al.* (*6*). Our measurements are in agreement with the results of this preliminary report, but our conclusion is different. The low-temperature measurements are absolutely necessary to detect the different Eu^{2+} sites.

2. $SrB_6O_{10}:Eu^{2+}$, Mn^{2+}

Samples $SrB_6O_{10}:Eu^{2+}$, Mn^{2+} were prepared to investigate the sensitizing action of Eu^{2+} on the Mn^{2+} emission. However, the Eu^{2+} ion is rather inefficient in this aspect. For example, for the composition $Sr_{0.98}Eu_{0.01}$ $Mn_{0.01}B_6O_{10}$ the relative amount of Mn^{2+} emission upon Eu^{2+} excitation is only a few percents at 4.2 K as well as at 300 K (Fig. 3). This result is not surprising since the Eu^{2+} I and Eu^{2+} II centers will transfer preferentially to the Eu^{2+} III center which has a corresponding allowed transition, while that of Mn^{2+} is strongly forbidden. The Eu^{2+}–Mn^{2+} transfer will be restricted to center III–Mn^{2+} transfer. However, this is expected to occur only over very short distance in view of the weak interaction (due to Mn^{2+}) and the unfavorable spectral overlap. The emission of Eu^{2+} III is situated at only slightly shorter wavelength than the Mn^{2+} emission. There-

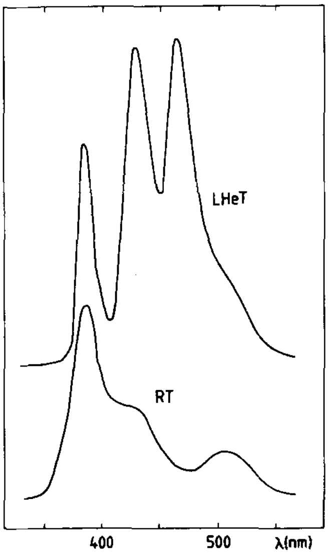

FIG. 3. The emission spectra of $Sr_{0.98}Eu_{0.01}$ $Mn_{0.01}B_6O_{10}$ at RT and LHeT (λ_{exc} = 300 nm).

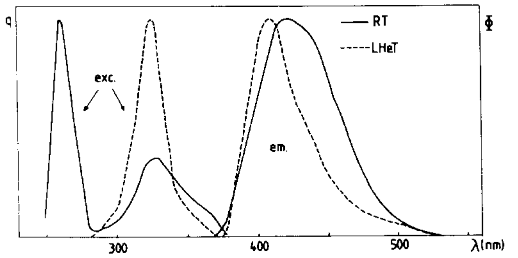

FIG. 4. The emission and excitation spectra of $Sr_{0.98}Sn_{0.02}B_6O_{10}$ at RT and LHeT.

fore, this transfer was not investigated further.

3. SrB_6O_{10}:Sn^{2+}

Figure 4 shows the emission and excitation spectra of SrB_6O_{10}:Sn^{2+} at 4.2 and 300 K. Figure 5 shows the temperature dependence of the decay time of the Sn^{2+} emission in the SrB_6O_{10} matrix. All decay curves were exponential, except for those below 15 K which show also a fast component (~10 μsec). The drawn curve gives a fit to a three-level scheme. If the levels are given by $1 > 2 > 3$, the fit yields $\Delta E_{32} = 36\ \mathrm{cm}^1$, $\tau_2 = 865$ μsec, and $\tau_3 = 5$ μsec. Here ΔE_{32} is the energy difference between levels 3 and 2 and τ_i denotes the radiative lifetime of level i (*7*).

Although not much work has been performed on Sn^{2+} luminescence in oxides at low temperatures, the interpretation of the results is straightforward. The two excitation bands corresponds to the $^1S_0 \rightarrow {}^3P_1$ and $^1S_0 \rightarrow {}^1P_1$ absorption transitions. As observed elsewhere, their energy difference amounts to about 1 eV (*8*). In view of the long decay time at low temperatures is ascribed to the $^3P_0 \rightarrow {}^1S_0$ transition which is strongly forbidden being a $0 \leftrightarrow 0$ transition. At higher temperatures the $^3P_1$ level is occupied and $^3P_1 \rightarrow {}^1S_0$ emission occurs. The corresponding radiative decay time is about 5 μsec which corresponds to the spin-selection rule which is only partly lifted in $5s^2$ ions.

Figure 4 shows that the emission and excitation spectrum show the same spectral shift with temperature, so that the occupation ratio of the $^3P_0$ and $^3P_1$ levels does not influence the spectra. This is due to the small value of ΔE_{32}.

The second, fast decay time at low temperatures is most probably related to the nonradiative $^3P_1 \rightarrow {}^3P_0$ transition. Comparable phenomena have been observed for Ga^+ in KBr (*9*). Our data are not accurate enough to allow further analysis.

It is interesting that the Sn^{2+} emission occurs mainly in one band, whereas the experiments with Eu^{2+} indicate the presence of several crystallographic sites for Sr^{2+}. The shape of the emission and excitation spectra (Fig. 4) shows that it is likely that there are several Sn^{2+} centers the spectra of which do not differ much. We are then left with the problem that the spectra of the different Eu^{2+} centers are strongly different, whereas those of the Sn^{2+} centers are more or less alike.

A probable explanation for this is the following. If we assume that the center of gravity of the excited $5d$ level of Eu^{2+} ions is the same for the three sites, and we make the same assumption for the $^3P_1$ level of Sn^{2+}, the crystal-field splitting of these levels should be very different. In fact, it is known that the crystal-field splitting of the

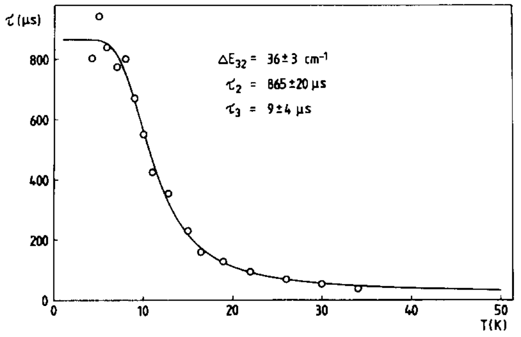

FIG. 5. Decay times of Sn^{2+} in SrB_6O_{10} as a function of temperature and the results from a three-level fit (solid curve).

$^3P_1$ level is only occasionally larger than 1000 cm^{-1} (*10*). The splitting of the 5*d* level of Eu^{2+}, however, is much larger (*11*), so that our results are explained if the sites are strongly different. A further analysis has to wait for a determination of the crystal structure of SrB_6O_{10}.

4. SrB_6O_{10}:Sn^{2+}, Mn^{2+}

It was shown before that Sn^{2+} in SrB_6O_{10} is a sensitizer of the Mn^{2+} emission (*1*). Figure 6 shows that the intensity ratio of the Sn^{2+} and Mn^{2+} emissions is not influenced by temperature. With these data we can make a further analysis of our previous results. First we note that the spectral overlap between Sn^{2+} emission and absorption is small which excludes Sn^{2+} → Sn^{2+} transfer. This is to be expected (*12*) in view of the absence of concentration quenching of the Sn^{2+} emission reported before (*1*). This implies that an excited Sn^{2+} ion can only emit its own emission or transfer to Mn^{2+} ions. Here we neglect nonradiative transitions in view of the high luminescence intensity. In this model the Sn^{2+} emission intensity and the Mn^{2+} emission intensity should increase with Sn^{2+} concentration. This was observed up till Sn^{2+} concentrations of 10 mole% (*1*). At higher concentrations there is obviously also some transfer to killers.

If we assume that the transfer from Sn^{2+} to Mn^{2+} covers *n* nearest lattice sites we find for low Mn^{2+} concentrations:

$$\frac{I(\mathrm{Sn}^{2+})}{I(\mathrm{Mn}^{2+})} = \frac{(1-c)^n}{1-(1-c)^n} \simeq \frac{1-nc}{nc}.$$

Here $I(X)$ denotes the emission intensity of the X emission and c the Mn^{2+} concentration. Therefore $I(\mathrm{Mn}^{2+})/I(\mathrm{Sn}^{2+})$ vs c should give a straight line for not too high values of c. This has also been observed (*1*). From these results we derive a value of $n = 12$. Since Sb^{3+} ($5s^2$) → Mn^{2+} transfer occurs by exchange (*13, 14*), we expect the same for the Sn^{2+} → Mn^{2+} transfer. This restricts the transfer to nearest and next-nearest neighbors. The value $n = 12$ seems to be a good estimate for this number of neighbors, but an accurate check has to wait for a crystal structure determination.

The weak temperature dependence of the transfer follows from Fig. 6. Here it is shown that the Sn^{2+} emission overlaps the Mn^{2+} absorption transitions favorably, so that the spectral overlap is only slightly temperature dependent. If the transfer is by exchange, no large temperature dependence is expected, in agreement with our observations.

Finally, we note that the Mn^{2+} emission band is rather broad which might be due to the presence of more than one Mn^{2+} center. This is in line with the results mentioned above, because the Mn^{2+} ion is expected to occupy the Sr^{2+} sites.

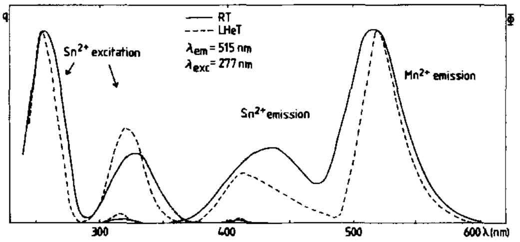

FIG. 6. The excitation and emission spectra of $Sr_{0.9}Mn_{0.07}Sn_{0.03}B_6O_{10}$ both at RT and LHeT.

5. SrB_6O_{10}:Pb^{2+}

Figure 7 shows the emission and excitation spectra of SrB_6O_{10}:Pb^{2+} at 4.2 and 300 K. In comparison with the Sn^{2+} luminescence the Stokes shift is much smaller in Pb^{2+}. Also the temperature dependence is different from that in the case of tin: the lead emission band shift to higher energy upon increasing temperature and the lead excitation band to lower energy.

Figure 8 gives the temperature dependence of the decay times of the Pb^{2+} emission. All decay curves were exponential. The drawn line gives the fit to a three-level

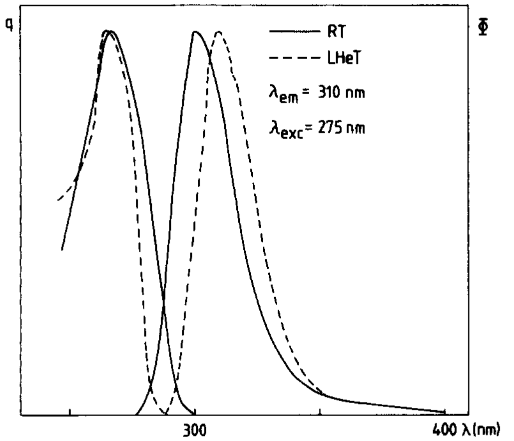

FIG. 7. The emission and excitation spectra of $Sr_{0.98}Pb_{0.02}B_6O_{10}$ at RT and LHeT.

scheme with ΔE_{23} = 1380 cm^{-1}, τ_2 = 52 μsec and $\tau_3 < 1$ μsec. The energy difference ΔE_{23} is relatively large and shows the the $^3P_1$ level is high above the $^3P_0$ level. This explains the thermal shift in Fig. 7. At 300 K the emission is from $^3P_1$, at 4.2 K from $^3P_0$. If we correct for the red thermal shift which follows from the excitation spectrum, we found for ΔE about 1500 cm^{-1}, which is in good agreement with the value obtained from the decay time measurements.

The shorter value of τ_3 in comparison with the Sn^{2+} is due to a further relaxation of the spin selection rule by increasing spin-orbit coupling. The value of τ_2 is expected be very long if the Pb^{2+} site symmetry would be cubic (*15*). Obviously the site symmetry under consideration is suitable to mix the $^3P_1$ and $^3P_0$ levels. A discussion of this effect has to be postponed until the crystal structure is solved. Further, it should be realized that the energy level scheme of s^2 ions can be more complicated than expected from simple theories (*2*).

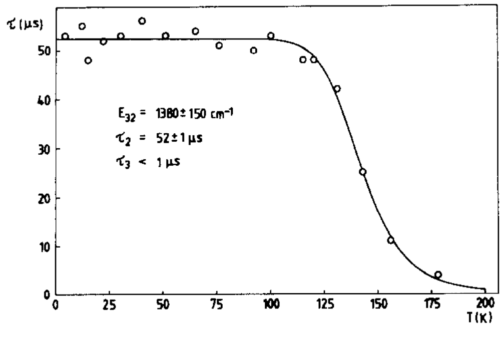

FIG. 8. Decay times of Pb^{2+} in SrB_6O_{10} as a function of temperature and the results from a three-level fit (solid curve).

In agreement with the Sn^{2+} spectra, those of Pb^{2+} do also not clearly indicate the presence of more than one Pb^{2+} center.

6. SrB_6O_{10}:Pb^{2+}

The Pb^{2+} ions sensitize the Mn^{2+} emission in SrB_6O_{10} also (*1*). The intensity ratio of the Pb^{2+} and Mn^{2+} emissions at 4.2 K for a given sample did not depend strikingly on temperature (Fig. 9). We will show now that the transfer characteristics of the codoped system SrB_6O_{10}:Pb^{2+}, Mn^{2+} are different from those in the tin manganese system. An essential data is the small Stokes shift of the Pb^{2+} luminescence which is responsible for a considerable overlap between emission and excitation spectra at 300 K (Fig. 7). Since the transitions involved are only slightly forbidden, this situation leads to a high Pb^{2+}–Pb^{2+} transfer probability. With the experimental spectral overlap and an oscillator strength of 0.1 the critical transfer distance is estimated to be about 20 Å (*1*, *3*). As an consequence, concentration quenching of the Pb^{2+} emission is observed above a few mole% of lead.

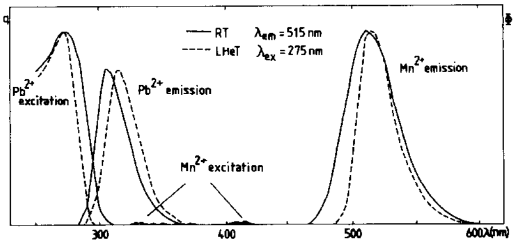

FIG. 9. The emission and excitation spectra of $Sr_{0.88}Mn_{0.04}Pb_{0.08}B_6O_{10}$ both at RT and LHeT.

Therefore, the intensity ratio of the Pb^{2+} and Mn^{2+} emission can be calculated with the fast diffusion model if the lead concentration is high. The expression is

$$\frac{I(Mn^{2+})}{I(Pb^{2+})} = \frac{c(Mn^{2+}) \cdot P_{Pb^{2+}-Mn^{2+}}}{c(Pb^{2+}) \cdot P_{Pb^{2+}}}.$$

Here $c(X)$ denotes the X concentration, $P_{Pb^{2+}-Mn^{2+}}$ the rate of energy transfer from lead to manganese, and $P_{Pb^{2+}}$ the radiative rate of the Pb^{2+} ion. Applying this to the data with 16% of lead (*1*) we found that $I(Mn^{2+})/I(Pb^{2+})$ vs $c(Mn^{2+})$ is a straight line as is to be expected and that $P_{Pb^{2+}-Mn^{2+}} = 16\ P_{Pb^{2+}}$. Since $P_{Pb^{2+}} > 10^6$ sec^{-1}, we have $P_{Pb^{2+}-Mn^{2+}} > 10^7$ sec^{-1}.

We conclude that the fast-diffusion model is valid and that the transfer in the lead-manganese systems is essentially different from that in the tin–manganese system due to the small Stokes shift of the Pb^{2+} emission. Now we turn to the weak temperature dependence of the Pb^{2+}–Mn^{2+} transfer. This suggests strongly that the fast diffusion model is still valid at 4.2 K, i.e., $P_{Pb^{2+}-Pb^{2+}} > P_{Pb^{2+}-Mn^{2+}}$. In view of the results for the Sn^{2+}-sensitized system and the spectra in Fig. 9, the temperature dependence of $P_{Pb^{2+}-Mn^{2+}}$ is expected to be small, that $P_{Pb^{2+}-Pb^{2+}}$ should be high at 4.2 K. However, if we have a look at Fig. 7 we note that the spectral overlap decreases drastically and vanishes. It should be realized that at 4.2 K the emission band corresponds to the $^3P_0 \rightarrow {}^1S_0$ transition and the excitation band to the $^1S_0 \rightarrow {}^3P_1$ transition, so that their spectral overlap is of no relevance.

We are interested in energy migration via the $^3P_1$ or via the $^3P_0$ level. The situation here is probably comparable to that described by Kellendonk *et al.* (*16*) for $YAl_3B_4O_{12}$: Bi^{3+}, i.e., the spectral overlap of the $^1S_0 \rightleftharpoons {}^3P_1$ transitions does not vanish at 4.2 K. Since $\tau_3 > \mu$sec and $^3P_0$ emission is observed, the $^3P_1 \rightarrow {}^3P_0$ nonradiative rate should be $>10^7$ sec^{-1}. If transfer occurs via the $^3P_1$ levels, the transfer rate should be even larger, i.e., $>10^8$ sec^{-1}. Since $P_{Pb^{2+}-Mn^{2+}}$ was found to be $>10^7$ sec^{-1}, the value for $P_{Pb^{2+}-Pb^{2+}}$ does certainly not exclude fast diffusion at 4.2 K, although it does not prove it either. Note, finally, that the considerations assume the presence of only one Pb^{2+} center which is not the case. Therefore, these estimated values have only a restrictive meaning.

Conclusions

The following concluding remarks can be made:

1. According to the luminescence spectrum of Eu^{2+} more than one type of Sr^{2+} ions seems to be present in SrB_6O_{10}. A crystal structure determination would be helpful for a more detailed discussion of the present results.
2. The Eu^{2+} ion does not sensitize the Mn^{2+} emission in SrB_6O_{10}, partly because $Eu^{2+} \rightarrow Mn^{2+}$ transfer is not very efficient, partly because the energy transfer occurs preferentially to one of the Eu^{2+} centers. This accepting Eu^{2+} center has a low quenching temperature, however.
3. The Sn^{2+} and Pb^{2+} ions acts as sensitizers for Mn^{2+} in SrB_6O_{10}, but they show different types of sensitization action. This is because $Sn^{2+} \rightarrow Sn^{2+}$ can be excluded whereas $Pb^{2+} \rightarrow Pb^{2+}$ transfer occurs. For the lead system a fast diffusion model seems to be valid.

Acknowledgments

The authors are indebted to Dr. P. A. M. Berdowski and Dr. G. J. Dirksen for the decay time measurements and for recording some of the low-temperature spectra. G. B. thanks the Dutch and Finnish Ministeries of Education for a fellowship. Financial aid from the Academy of Finland (M.L.) and Foundation of Technology in Finland (T.K.) is gratefully acknowledged.

References

1. T. Koskentalo, M. Leskelä, and L. Niinistö, *Mater. Res. Bull.* **20,** 265 (1985).
2. C. W. M. Timmermans and G. Blasse, *J. Solid State Chem.* **52,** 222 (1984).
3. D. L. Dexter, *J. Chem. Phys.* **21,** 836 (1953).
4. G. Blasse, *Philips Res. Rep.* **24,** 131 (1969).
5. K. C. Bleijenberg and G. Blasse, *J. Solid State Chem.* **28,** 303 (1979).
6. K. Machida, G. Adachi, and J. Shiokawa, *J. Lumin.* **21,** 101 (1980).
7. G. Boulon, C. Pedrini, M. Guidoni, and C. Pannel, *J. Phys. (Les Ulis, Fr.)* **36,** 267 (1975).
8. A. Ranfagni, D. Mugnai, M. Bassi, G. Viliani, and M. P. Fontana, *Adv. Phys.* **32,** 823 (1983).
9. D. Le Si Dang, R. Romestain, O. Simkin, and A. Fukuda, *Phys. Rev. B* **28,** 2989 (1978).
10. A. C. van der Steen, J. J. A. van Hesteren, and A. P. Slok, *J. Electrochem. Soc.* **128,** 1327 (1981).
11. G. Blasse, W. L. Wanmaker, J. W. ter Vrugt, and A. Bril, *Philips Res. Rep.* **23,** 189 (1968).
12. R. C. Powell and G. Blasse, *Struct. Bonding (Berlin)* **42,** 43 (1980).
13. T. F. Soules, R. L. Bateman, R. A. Hewes, and E. R. Kreidler, *Phys. Rev. B* **7,** 1657 (1973).
14. G. Blasse, *Chem. Phys. Lett.* **104,** 160 (1984).
15. A. C. van der Steen and L. T. F. Dijcks, *Phys. Status Solidi B* **104,** 283 (1981).
16. F. Kellendonk, T. van den Belt, and G. Blasse, *J. Chem. Phys.* **76,** 1194 (1982).